Article ID: 1006-8775(2011) 03-0257-11

APPLICATION OF WRF/UCM IN THE SIMULATION OF A HEAT WAVE EVENT AND URBAN HEAT ISLAND AROUND GUANGZHOU

MENG Wei-guang (蒙伟光)[1, 2], ZHANG Yan-xia (张艳霞)[1], LI Jiang-nan (李江南)[3], LIN Wen-shi (林文实)[3], DAI Guang-feng (戴光丰)[1], LI Hao-rui (李昊睿)[1]

(1. Guangzhou Institute of Tropical and Marine Meteorology, CMA, Guangzhou 510080 China; 2. State Key Laboratory of Severe Weather, Chinese Academy of Meteorological Sciences, Beijing 100081 China; 3. School of Environmental Science and Engineering, Sun Yat-sen University, Guangzhou 510275 China)

Abstract: This paper evaluated the performance of a coupled modeling system, Weather Research and Forecasting (WRF)/Urban Canopy Model (UCM), in the simulation of a heat wave event which occurred around Guangzhou during late June through early July, 2004. Results from three experiments reveal that the UCM with new land data (hereafter referred to as E-UCM) reproduces the best 2-m temperature evolution and the smallest minimum absolute average error as compared with the other two experiments, the BPA-Bulk Parameterization Approach with new land data (E-BPA) and the UCM with original U.S. Geological Survey land data (E-NOU). The E-UCM is more useful in capturing the temporal and spatial distribution of the nighttime Urban Heat Island (UHI). Differences in surface energy balance between the urban and suburban areas show that low daytime albedo causes more absorption of solar radiation by urban areas. Due to the lack of vegetation which inhibits cooling by evapotranspiration, most of the incoming energy over urban areas is partitioned into sensible heat flux and therefore heats the surface and enhances the heat wave. During nighttime, the energy in the urban area is mainly from soil heat flux. Although some energy is partitioned as outgoing long wave radiation, most of the soil heat flux is partitioned into sensible heat flux due to the small latent heat flux at night. This leads to the development of nighttime UHI and the increase of the magnitude and duration of heat waves within the municipality.

Key words: heat wave; Urban Heat Island (UHI); Urban Canopy Model (UCM); numerical simulation

CLC number: P423 **Document code:** A **doi:** 10.3969/j.issn.1006-8775.2011.03.007

1 INTRODUCTION

It is generally held that the formation of high-temperature weather is immediately associated with governing factors induced by anomalous atmospheric circulation, such as warming from advection transfer, diabatic descending motion and clear-sky radiation[1, 2]. Apart from these factors, high-temperature weather in urban areas may also be more closely related to the joint effect of its particular structure of the underlying surface with man-made heat emission. As shown in some preliminary research results[3, 4], the warming effect triggered by UHI can result in the increase of extreme high-temperature weather in cities. It is then necessary to study this phenomenon with much focus.

The term "UHI" originates from Manley[5] in 1958, when it was used to describe the phenomenon that urban atmosphere and its underlying land surface experience higher temperatures than its suburban districts. As the urbanization effect is related to clouds, precipitation and air quality in the urban and neighboring areas and even the issue of global warming, in addition to its role in the distribution and variation of temperature, its study receives more and more attention in recent years[6] and the data and methods employed in the study are more and more advanced. Specifically, owing to the application of modern means of observation, like satellite remote-sensing, some facts have been revealed in greater detail on the effect of urbanization on the environmental atmosphere[7] and three-dimensional

Received 2010-06-25; **Revised** 2011-05-20; **Accepted** 2011-07-15
Foundation item: Natural Science Foundation of China (40775068); Specialized Projects of Scientific Research for Public Welfare Industry (Meteorology); Open Projects of Key National Laboratories for Disasters-causing Weather (GYHY200706014; GYHY200906026); Science Foundation of China (2009LASW-B03); Foundation for Scientific Research on Tropical and Marine Meteorology
Biography: MENG Wei-guang, associate professor, primarily undertaking research on mesoscale tropical meteorology and numerical simulation.
Corresponding author: MENG Wei-guang, e-mail: wgmeng@grmc.gov.cn

techniques of simulation and forecasting, with the urban effect included, have been so developed that they become a powerful means for extensive investigation into this issue[8, 9].

Due to the ability to provide spatiotemporal variations of the UHI, numerical models have been used effectively to work on this phenomenon. Earlier UHI models proposed are mostly one-dimensional, land-surface models with equilibrium energy, based on which an early work was done on the UHI by Myrup[10], which concluded that the lack of water in the land surface and relatively large thermal inertia in the urban area are two important factors leading to the development of UHI. It is, however, hard for such models to reproduce the observational fact that the UHI appears at nighttime as they do not take care of the effect of advection, saying nothing of the urban canopy (i. e. the atmospheric layer closest to the urban land surface that is as thick as the average height of all the buildings within a city), such as the geometric features of buildings. A two-dimensional (on the vertical plane) model for urban boundary layers (URBMET) was once used to study the effect of different types of cities by Bornstein[11] in separate discussions of the effects of three types of cities with rough, warm and rough/warm conditions on the environmental field. A three-dimensional model put forward by Vuovich et al.[12] in 1976 was the first of its kind to address the urbanization issue. Utilizing a primitive-equations static model they had developed, they focused their attention on the effect of St Louis, U.S.A. on the environmental flow field but did not make much effort in revealing the evolution of the UHI. Afterwards, three-dimensional models were used more and more widely in studying the urban effect. Examples of this include Yosikado[13] and Schayes et al.[14] The former used a three-dimensional numerical model to study the urban environment of Tokyo, Japan and its interactions with sea breeze, and the latter improved the URBMET model of Bornstein to turn it into a three-dimensional model, URBMET/TVM, that takes into account terrain effects, which was used to study the phenomenon of sea-breeze fronts intrigued by cities and topographic features in New York. In addition to these models specifically developed and applied for the research on urban environment, mesoscale numerical prediction (NWP) models—aiming at how to better describe the UHI—have also become an important part of the model forecasting techniques. Some of the leading mesoscale models, such as Mesoscale Model version 5 (MM5) and Regional Atmosphere Modeling System (RAMS), are all capable of simulating complicated urban underlying surface. Mainly through a coupled Noah Land Surface Model (Noah LSM), the MM5 depicts the effect of urban conditions by fine-tuning the overall urban parameters like reflectivity and roughness, while the RAMS takes into account the role of urban canopy in its processing of land-surface processes[8, 15].

As the urban canopy has the most immediate influence on the urban boundary layer, coupling an urban canopy model (UCM) in mesoscale models for describing in greater detail the thermodynamics and dynamics of cities has been very important in the development of model forecasting techniques. Apart from the RAMS, the Weather and Research Forecasting (WRF) model, currently in wide use, has its Noah LSM coupled with a corresponding UCM[9]. As compared to some land surface models (which are introduced above), these UCM models have improved the description of urban thermodynamic and dynamic effects and the simulation of thermal storage effect, flow field and precipitation distribution, as they incorporate the buildings' role in blocking radiation and reflecting shortwave and longwave radiation[15-17].

In this paper, the mesoscale WRF model and the UCM model are used to simulate the formation of a high-temperature weather in the area of Guangzhou and investigate the properties of WRF/UCM models and their effects on the simulations of UHI and the high-temperature weather. The case for study is a process of high-temperature weather that occurred over most of Guangdong in late June to early July in 2004. The high-temperature sustained as the province was under the joint effect of the subtropical high and periphery circulation around Typhoon Mindulle. According to the meteorological record, 22 observation stations in Guangdong broke their local records of maximum temperature during June 29th–July 1st, with the highest temperature at 39.8° C. In Guangzhou, the highest temperature stayed above 38° C for three days running and its highest measurement (39.3° C) made it surpass the historical record in the municipality.

2 SUMMARY OF THE HIGH-TEMPERATURE IN GUANGZHOU IN THE SUMMER OF 2004 AND BACKGROUND

There has been much work on the weather of high temperature in Guangzhou[18-20]. As shown in the statistics, nearly 96% of the high-temperature weather in Guangzhou is related to the effect of typhoons and the subtropical high[18]. Being a typical high-temperature weather, it occurred when the periphery circulation around Typhoon Mindulle co-acted with the subtropical high in the West Pacific. In late June, 2004, Mindulle was formed over the waters around the Philippines before heading northwest to move into the Bashi Channel on June 29th. Then, the typhoon turned to move to the north as it was steered by a southerly flow from a deep trough connected with a stationary trough over East Asia. It made two successive landfalls, first in eastern Taiwan

on July 1st and then in coastal Zhejiang on July 3rd. Instead of receiving winds and rain as a result of the typhoon, much of the southern China experienced a sustained span of high temperature due to extended duration at the periphery of the storm and continuous dominance of the subtropical high. Fig. 1 shows the distribution of geopotential height and wind fields at 500 hPa, available based on a 1° ×1° National Centers for Environmental Prediction (NCEP, USA) reanalysis dataset, for 0800 (Beijing Standard Time, same below) 1 July, 2004. It is clearly shown in the figure that the eye was then close to southeastern Taiwan while the subtropical high circulation, split up to Mindulle's northwest, still controlled the whole of southern China. It was under the joint effect of the subtropical high and the descending airflow at the storm's periphery that the high-temperature weather occurred over most of the province. Fig. 2 gives the cross section of the vertical circulation across the line of $\overline{AB}$ in Fig. 1. It shows more clearly that a descending airflow was prevailing below the level of 850 hPa over Guangzhou and the area west of it, which was conducive to the stability of atmospheric stratification and sustained rise of air temperature.

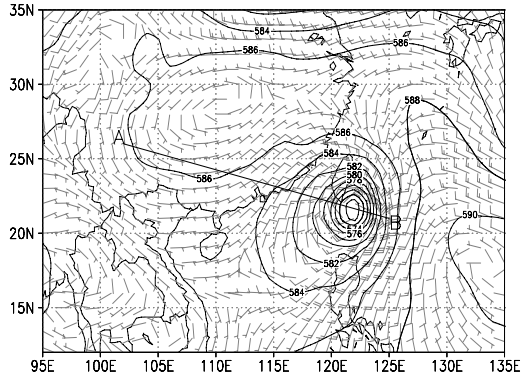

Fig. 1. 500-hPa geopotential height and wind fields for 0800 BST 1 July 2004.

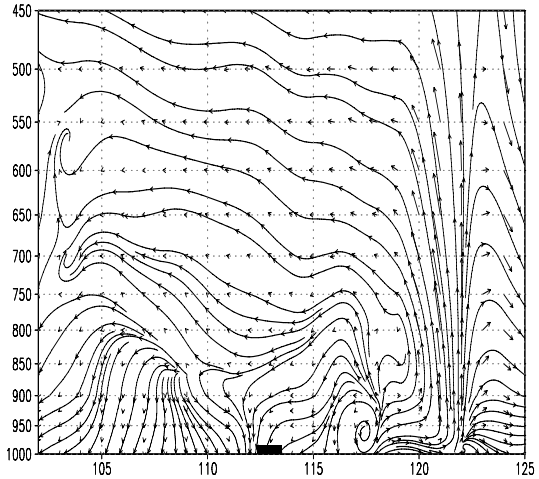

Fig. 2. Cross sections of the vertical circulation across the line of $\overline{AB}$ in Fig. 1; the black rectangular near 113.3° E is where Guangzhou is located.

Figure 3 presents the evolution of temperature for an automatic weather station (AWS, coded G1001) at Tianhe, Guangzhou for the time from 0800 BST June 21st to 0800 BST July 4th, 2004. The figure shows that the maximum temperature surpassed 35° C, starting from June 27th, for seven days in a row; it was above 38° C from June 29th to July 1st, with the highest at 39.3° C, breaking the historical record of maximum temperature in Guangzhou. Apart from the daytime maximum temperature, the minimum temperature also rose during the night in this city and stayed above 31° C from the night of June 30th to the early morning of July 1st. Fig. 4 shows the comparison of temperature evolution between urban Guangzhou (represented by AWS G1001) and the suburban area (represented by AWS G1064 in Conghua County), which are about 50 km apart from each other. The figure clearly indicates well-defined UHI features in the urban area as well as the high-temperature characteristics. Temperature contrasts are increasing during the nighttime, especially after sunset, between the urban and suburban districts of Guangzhou, with the maximum difference of temperature being more than 5° C and the average difference being more than 2° C. During the daytime, the temperature difference can be negative at some time, similar to some findings of existing studies. As found in observational studies, the intensity of UHI increases after sunset and attains its maximum level at some point before sunrise. It is relatively weak during the day and turns to its opposite by becoming a "cool island", something that may be related to the sun-blocking effect by high-rise buildings in the urban area and the effect of urban aerosol emission on shortwave radiation[21].

3 NUMERICAL MODEL AND DESIGN OF EXPERIMENT SCHEME

The numerical model used in our simulation study is WRFV2.2. Prior to this version, the Noah LSM is used to describe the urban effect in models by adjusting the parameters about urban districts (like the reflectivity and roughness) in model gridpoints, i.e., by means of Bulk-Parameterization Approach (BPA). Starting from V2.2, however, Kusaka et al.[9] coupled a single-layer UCM model with the WRF model. One of the basic goals of this UCM model is to have a better description of the role of urban geometric features in land-surface energy equilibrium and wind shear. The model takes into account, though briefly, the geometric features of buildings and roads to depict the blocking, intercepting and reflecting effects of urban canopy on the wind shear as well as on shortwave and longwave radiation, and calculates the heat transfer taking place at the top of the buildings, bodies of

wall and road surfaces on individual basis. See Kusaka and Kimura[22] for this UCM model.

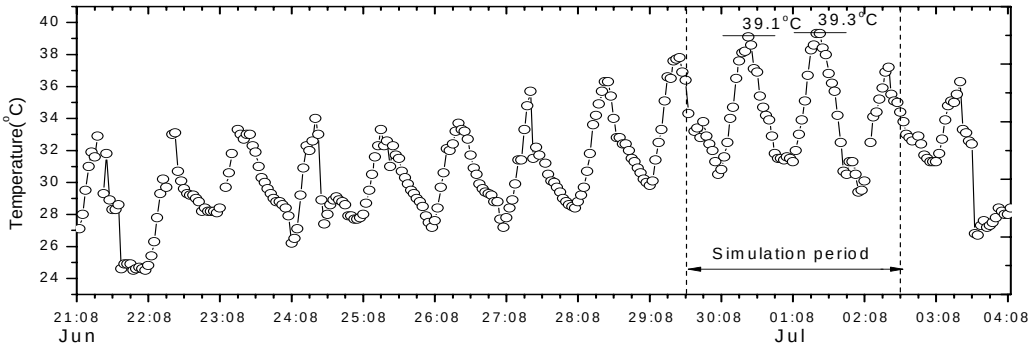

Fig. 3. Evolution of temperature at AWS G1001 at Tianhe, Guangzhou from 0800 BST June 21st to 0800 BST July 4th, 2004 (abscissa: time).

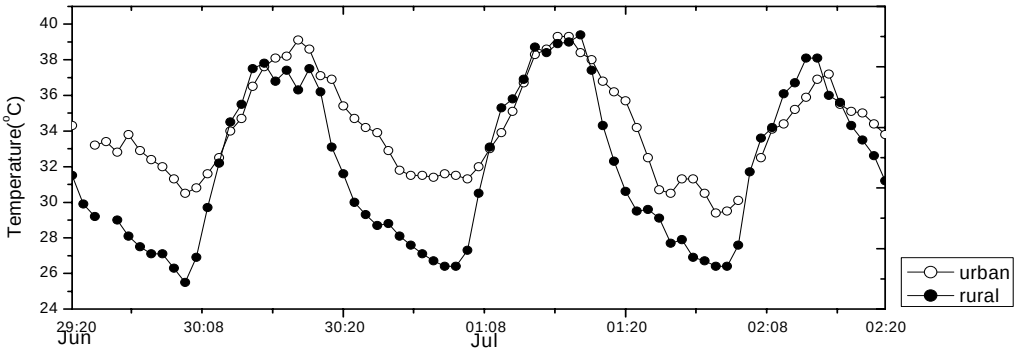

Fig. 4. Comparisons of the evolution of temperature over urban Guangzhou (curve with hollow circles) and its suburban districts (curve with solid circles) from 2000 BST June 29th to 2000 BST July 2nd (abscissa: time).

It is advisable to have access to detailed local land-use data when applying the UCM model. In this model, three types of land use, low-density residential area (Type 31), high-density residential area (Type 32) and commerce / industry / communications (Type 33), are set up for urban areas. The parameters related to urban areas are specifically assigned according to the real situation. In our study, a high-resolution geographic information system (GIS) dataset on the land use in Guangdong province, available at present, is used to categorize the residential, township and manufacturing/mining uses of the land according to the three types presented above, and then the land use data are incorporated into the WRF model. Fig. 5 shows the regional setup of the simulation study. With the introduction of the GIS dataset, the data are both applied in domains D01 and D02. Domain D02 shows the urban development of Guangzhou and neighboring areas where red color represents the land of cities and towns. The yellow and blue colors are associated with the land for residential use at the sub-township level and industry/communications/construction, respectively. Of course, such one-for-one matching is still too simple to fully describe the difference in land use; it needs to introduce more detailed land-use data in our future study.

To understand how well the WRF/UCM simulates the UHI and high-temperature weather in urban environment, three experiments were designed for situations with or without the UCM model and with the new or old data of land use (Table 1). The first experiment (E-UCM) explicitly processes relevant urban effects by employing the newly incorporated land-use data and using the Noah LSM as its land-surface process model that couples with a UCM model. The second experiment (E-BPA) still uses the aforementioned overall parameterization method to describe the urban effects. Through comparisons and analysis of the results of the two experiments, the performance of the UCM and its simulating capabilities for high-temperature weather can be examined. For deeper probe into the effect of UHI on high-temperature weather, a third experiment (E-NOU) is designed. In addition to the data of land use types in the model domain that still uses the 30′ data from the U.S. Geological Survey (USGS) available in the original model, other details of design are the same as those of the E-UCM. As the 30′ data of USGS are developed based on 1992/1993 NDVI of satellites, the urban districts of Guangzhou and other cities in the Pearl River Delta described are much smaller than they are now. From this difference of simulations between the two experiments, the effect of urban development on high-temperature weather is shown.

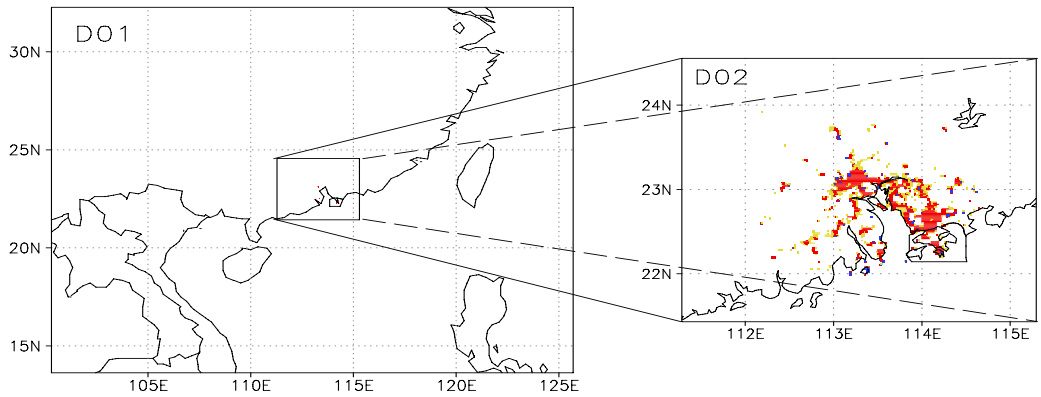

Fig. 5. Setup of the domain for simulation study and the development of Guangzhou and neighboring cities.

Table 1. Design of the experimental scheme for simulation.

Names	Land process schemes	Land use	Model of urban canopy
E-UCM	Noah LSM	GIS dataset	Included
E-BPA	Noah LSM	GIS dataset	Not included
E-NOU	Noah LSM	USGS 30′	Included

According to the design, all of the three experiments are run in doubly nested grids (Fig. 5). With grid intervals at 15 km and 3 km for D01 and D02, respectively, the model has 35 layers vertically. It starts the integration from 2000 BST on June 29, 2004 for a span of 72 hours. The initial and boundary conditions are provided by the 1° ×1° National Centers for Environmental Protection (NCEP, USA) Final Analyses (FNL) data. Other physical schemes include: WM-3 ice-phased microphysics scheme, Dudhia shortwave radiation scheme, and RRTM longwave radiation scheme. While no cumulus convection scheme is used for the inner layer of the model, the Kain Fritch cumulus convection scheme is applied for the outer layer. All three experiments use the YSU scheme in the boundary layer. Throughout the integration, the outer model layer assimilates the FNL gridpoint analysis once every six hours using the four-dimensional nudging available with the WRF model itself. This study mainly discusses the simulations of the inner layer.

4 ANALYSIS OF THE SIMULATIONS

4.1 *Comparisons of the simulations from the three experiments*

Figure 6 presents the urban temperatures simulated in the three experimental schemes (indicated with the temperature at the height of 2 m at the location of the AWS G1001 in Guangzhou) and compares them with the observations. Due to the model's spin-up issue in the first 10 hours, which resulted from direct interpolation of the NCEP reanalysis to determine the initial conditions, the three experiments all yielded simulations that differ much from the observations. 10 hours later, however, all of the experimental schemes have better reproduction of the diurnal variation of temperature, though with varying magnitudes. A statistical analysis of the simulations after the 10th model hour has shown that on average, the E-UCM simulation has an absolute error of 1.01° C, EBPA 1.19° C, and E-NOU 1.71° C, respectively. Temporally, the E-UCM experiment is the best in reproducing the variation of urban temperatures, with the maximum daytime temperature it simulates being the closest to reality; it reflects the nighttime characteristics as well by simulating relatively high minimum temperature in the urban district. It is the key to whether or not a model can be successful in reproducing the UHI features. Compared with the E-UCM, E-BPA has lower daytime maximum temperature and nighttime minimum temperature, though it does, to some extent, enhance the description of the urban effect. Compared with the other two experiments, the E-NOU experiment produces simulations that deviate the most from the observations, as evidently shown by much lower maximum temperatures for the day and much lower minimum temperatures for the night. It is caused by the lack of realistic description of urban land use in the simulated domain.

4.2 *Improvement of UHI simulations by WRF/UCM*

By comparing the simulations of the three experiments, the simulating capabilities of the UCM can be examined further. Fig. 7 presents the evolution of the heat island intensity as simulated by the three experiments and its comparison with the observations. The intensity of the heat island effect is represented by the difference in temperature at the 2-m height between AWS G1001,

for urban districts, and G1064, for suburban districts, as mentioned in previous sections. As shown by the observations, the heat island intensity is gradually increasing after midday and becomes strongest at night, with the maximum temperature difference at more than 5° C, while it gradually decreases in the morning and even gets negative at noon. Though none of the experiments reproduces these characteristics of the heat island evolution, especially those in the daytime, the E-UCM experiment, coupled with the UCM model, did improve the simulations to some extent so that relatively intense nighttime heat island was reproduced, while neither the E-BPA nor E-NOU experiments could due to their incomplete description of the urban effect. Take June 30th and the night of July 1st for instance. The intensity of the heat island effect is around 3° C, much better than that simulated by either the E-BPA or E-NOU experiments.

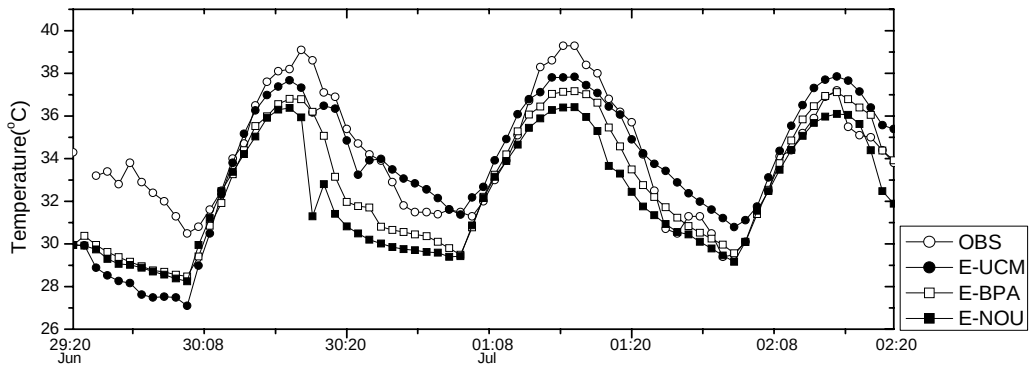

Fig. 6. Evolution of urban temperatures simulated in the three experimental schemes from 2000 BST June 29th to 2000 BST July 2nd and their comparisons with the observations (curve with hollow circles).

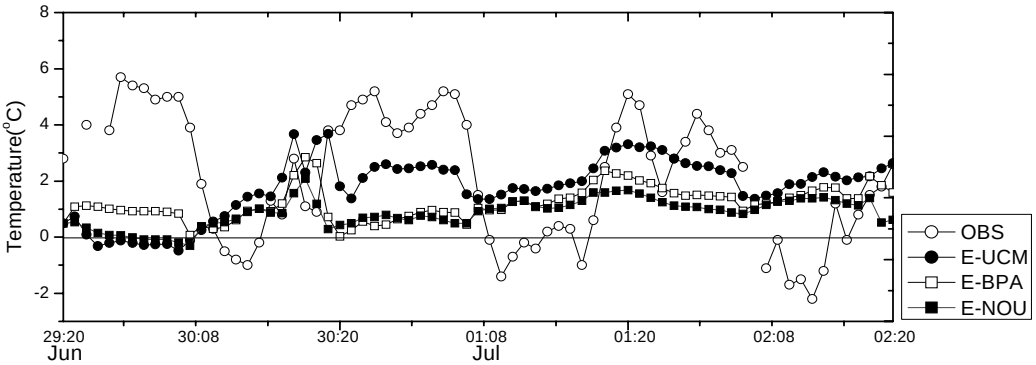

Fig. 7. Same as Fig. 6 but for the heat island intensity.

In addition to the improved simulations of the heat island intensity, the E-UCM experiment also did a good job in simulating the distribution of the heat island effect. Fig. 8 shows the distribution of 2-m temperatures in Guangzhou analyzed from the AWS observations and simulated by the three experiments for 2300 BST June 30th when the heat island effect evolved significantly at the time of the day. As shown in analysis of observational data (Fig. 8a), the heat island effect of Guangzhou is mainly distributed to its west and southwest in Foshan with the core shaped like a stripe orienting northeast-southwest and the maximum temperature at 32° C, corresponding to the urban districts (as indicated by grey shade in the figure). Besides, the heat island effect is also obvious in the urban districts of southeastern Guangzhou and Dongguan. When drawn with an isotherm of 31° C, the cities can be well identified for their role in the formation of heat island effects. Except for Shenzhen where temperatures higher than 31° C do not occur possibly due to oceanic modulation, all of the urban areas of the Pearl River Delta (Guangzhou, Foshan, Dongguan etc.) are within the coverage of the 31° C isotherm. The results of the E-UCM, as given in Fig. 8b, show that the application of the UCM model can well simulate the characteristics of a nighttime heat island. As compared to Fig. 8a, although the area covered by the 31° C isotherm is larger, there are many other similarities in distribution. For instance, the core of the heat island simulated by E-UCM is also located over Guangzhou, Foshan and Dongguan, and the locations with higher temperatures in the heat island are over the urban districts where temperatures are 32° C and higher. Compared with the simulations by E-UCM, the heat island reproduced by E-BPA is corresponding to where the urban parts are, but with much smaller

coverage, weaker intensity, and a maximum temperature of less than 32° C at the core (Fig. 8c).

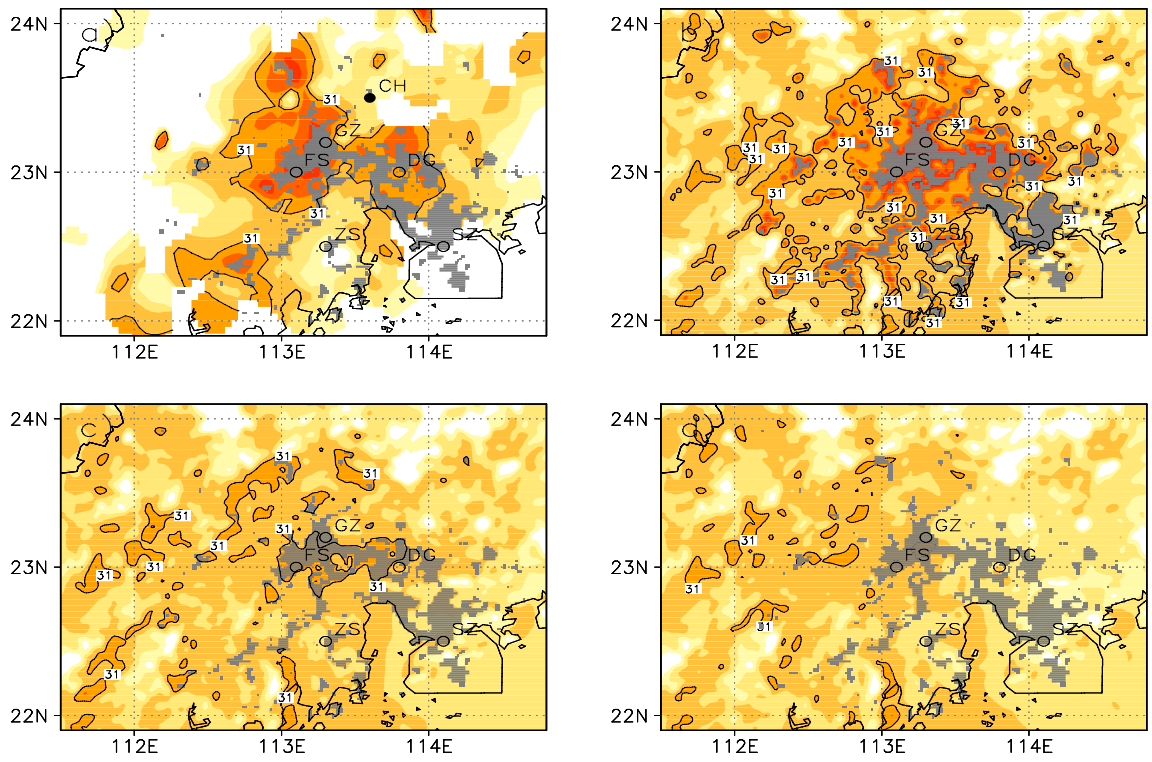

Fig. 8. Distribution of 2-m temperatures analyzed from the AWS observations and simulated by the three experiments for the time of fullest evolution of heat island effects at 2300 BST June 30th. a: Observational analysis: b. E-UCM; c: E-BPA; d: E-NOU. The shades stand for the urban areas of Guangzhou and the Pearl River Delta. Cities are located where the "○" is. GZ: Guangzhou; FS: Foshan; DG: Dongguan; ZS: Zhongshan; SZ: Shenzhen. Observation stations representing the suburban areas are indicated by "●". CH: Conghua

It needs to be pointed out that the E-UCM still has errors in its simulations of the urban temperature close to the sea, like the more-than-31° C temperatures in the area of Shenzhen, higher than the observation. It points to some difficulty concerning the UCM's correct simulation of temperature changes in coastal urban districts possibly due to the lack of sufficient capabilities of the model in simulating the oceanic modulation, though it improves lower-than-reality simulations of nighttime urban temperatures. As shown in Fig. 8d, the relatively small boundary of cities with the E-NOU experiment has resulted in non-existence of any heat island.

5 FORMATION OF URBAN HEAT ISLANDS AND THEIR ROLE IN HIGH-TEMPERATURE WEATHER

There are multiple reasons in play to affect the formation of urban heat islands. According to Oke[23], urban buildings—having higher temperatures at night—keep blocking the sky, contributing mainly to the maintenance of temperatures warmer than the surroundings. During the night, land surface loses heat through radiative cooling while the existence of buildings prevents it from happening. Besides, reduced urban vegetation and altered thermal properties at land surface are also important input; building materials used in cities, such as cement and asphalt, differ substantially in thermal properties (including thermal capacity and thermal conductivity) as compared to the suburb. Differences also occur in the radiation traits of the urban land surface, e.g., rates of reflectivity and emission. All of these may result in changes in land-surface equilibrium of energy in cities to lead to higher temperatures in the urban than suburban areas.

On the other hand, the geometric features of cities are also attributable to the formation of the UHI. Making available multiple interfaces for reflection and absorption of solar rays, urban buildings enhance the effect of heating over cities. Another effect of the buildings is the blocking of winds. As calm conditions are conducive to stable stratification, convection-induced cooling is inhibited from taking place. Besides, the exhaust heat discharged from automobiles, air-conditioners and industries also contribute to the forming of UHI. Moreover, as a number of pollutants are capable of altering the radiative properties of the atmosphere, high-level emission of urban pollutants is also

playing a role in the intensity of the UHI.

The causations of the UHI—though as multiple as what has been presented above—need to be represented in models as contributing factors during energy equilibrium processes for land surfaces. Through comparisons and analysis of these processes between experiments and between urban and suburban areas, knowledge about how the model-shown UHI forms can be obtained. The locations of the urban and suburban areas follow the same captions presented above. To focus on the formation of UHI on June 30th, Fig. 9 gives the temporal evolution of constituting components in the urban area of the land-surface energy equilibrium during a E-UCM experiment from 0300 BST June 30th to 0300 BST July 1st (in which positive values denote input, and negative values stand for output, of energy). Here, the incoming solar shortwave radiation is expressed as absorption of energy, i.e., it has taken into account the reflecting effect of urban areas. It is then clear that the input of energy is mainly from the absorption of solar shortwave radiation as the source of energy while the sensible- and latent-heat flux and soil heat flux are output as the sink of energy. At night, the thermal flux of soil acts as input to become a main source of energy while the flux of sensible heat, though much smaller than during daytime, remains negative as it keeps outputting energy to heat the atmosphere.

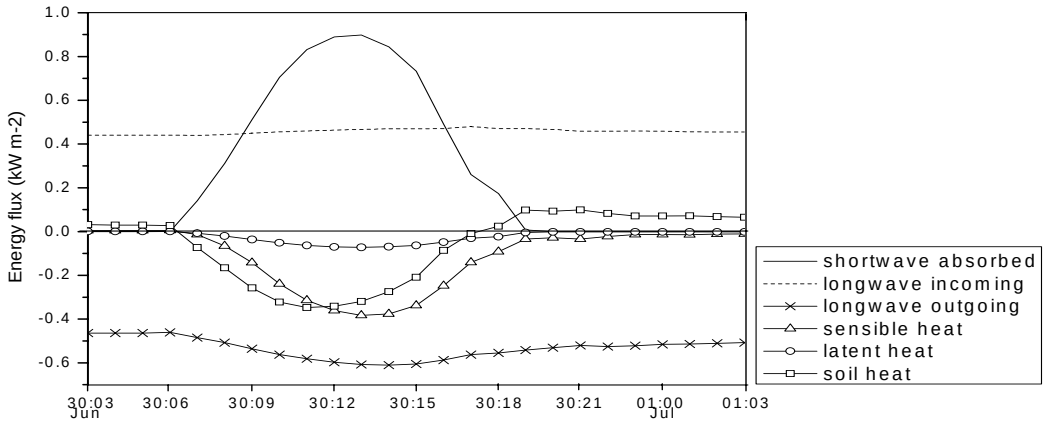

Fig. 9. Temporal evolution of constituting components in the urban area of the land-surface energy equilibrium during a E-UCM experiment. Unit: kW/m^2; abscissa: time

All but the term of shortwave-radiation absorption have relatively large soil heat flux and sensible heat flux, with the maximum appearing at noon at -0.35 and -0.38 kW/m^2, respectively. During the daytime, soil heat flux propagating downward is almost in-phase with the absorption of shortwave radiation while sensible heat flux is lagging behind it by 1 to 2 hours and remains negative even after sunset. Having a small magnitude, latent heat flux—being only -0.07 kW/m^2 at maximum—loses heat diurnally owing to evaporation, which is absent nocturnally. Having large magnitudes, longwave radiation—pointing both upward and downward—are the two terms that change little in daily variation; the upward longwave radiation is generally larger than the downward radiation with the difference being the largest at midday, around 0.14 kW/m^2.

Figure 10 presents the differences in the energy equilibrium between the urban and suburban areas with the UCM experiment (Fig. 10a), and differences in the energy equilibrium between the E-UCM nd E-BPA (Fig. 10b) and between the E-UCM and E-NOU (Fig. 10c), respectively, for urban areas. As shown in Fig. 10a, the UCM experiment shows higher diurnal absorption of shortwave radiation in the urban than suburban areas, owing to smaller reflectivity of the former (10%), a populated residential area (Type 32 in land use), than the latter (18%), irrigated farmland/grassland (Type 3). As a result, the E-UCM absorbs more shortwave radiation over the urban area. Differences are small in the term of downward longwave radiation between these areas, affecting simulations only mildly. The largest difference between them is the diurnal latent heat flux, which can be higher than 0.4 kW/m^2, at noon, while remaining small at night. It suggests much smaller diurnal latent-heat flux in the urban than suburban area, a characteristic that relates closely to little vegetation and lack of evapotranspiration in the urban area. The second largest difference occurs with the flux of sensible heat and latent heat, with the urban area having larger flux than the suburban area, mainly during the daytime and greater than -0.25 kW/m^2. After sunset, the difference in soil heat flux turns from negative to positive while that of latent heat flux stays in the negative territory. At its maximum, the upward longwave radiation is also marked with a difference of more than -0.05 kW/m^2.

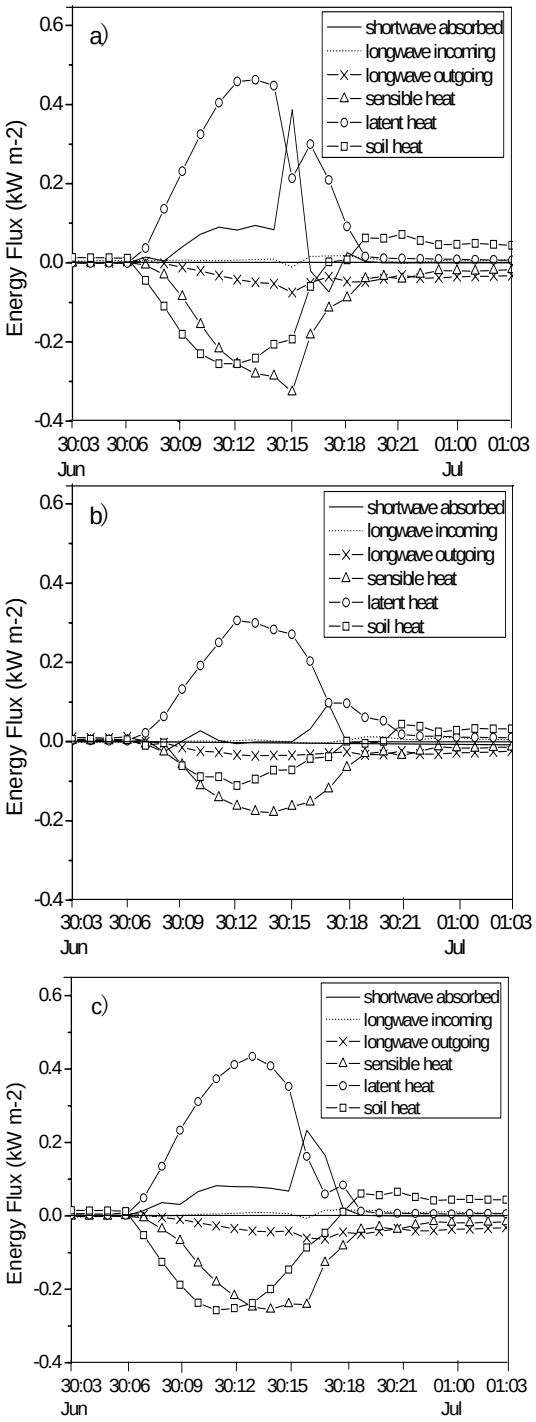

Fig. 10. Differences in the energy equilibrium between the urban and suburban areas with the UCM experiment (a), and differences in the energy equilibrium between the E-UCM nd E-BPA (b) and between the E-UCM and E-NOU (c), respectively, for urban areas.

From the differences between individual terms of energy equilibrium and their evolutions, it can be determined that high diurnal temperatures in urban areas are linked with reduced reflectivity and increased absorption of shortwave radiation there. Due to the lack of evapotranspiration and small latent heat flux in urban areas, most of the increased shortwave radiation heats up the atmosphere in the form of sensible heat while the remainder is consumed in increasing the downward-going soil heat flux. Besides, for this particular process of high-temperature weather, the stratification was stable—thanks to the effect of the subtropical high and descending airflow at the periphery of the typhoon—in the levels near the surface, probably causing larger temperature rise and contributing, effectively, to the formation of diurnal high-temperature weather. At night, the land surface obtains its energy mainly from upward-going soil heat flux as solar shortwave radiation reduces to zero.

The difference of the nocturnal term is positive, as shown in Fig. 10a, suggesting more upward-transporting soil heat flux in the urban than suburban area, with the maximum larger than 0.06 kW/m^2. Likewise, as the urban latent heat flux is small and the input of energy is mainly spent on increasing sensible heat, the difference in nocturnal sensible heat shows that urban sensible heat continues into the night, playing a substantial role in maintaining higher temperatures in cities. Of course, some of the increased soil heat flux is assigned to be used to increase the upward longwave radiation in addition to enhancing sensible heating and the negative difference in the upward longwave radiation suggests stronger radiative cooling. It is somewhat contradictory to the analysis of Oke[23]. It deserves more detailed work on ways to describe the effect of buildings intercepting longwave and shortwave radiation. Besides, anthropogenic heat release, another source of nocturnal energy input, is not considered in the model, which may affect the correct description of the equilibrium of nocturnal longwave radiation.

Figure 10b gives the differences between individual terms of energy equilibrium over cities, which shows the improvements made to the model when the urban canopy is included. Similarly, the largest difference lies in the diurnal latent heat flux, i.e., the urban latent heat flux is reduced with the E-UCM if it is compared to the E-BPA. In addition, both the sensible heat flux and soil heat flux with the E-UCM are larger diurnally than the E-BPA and the difference in sensible heat flux of both experiments is still negative after sunset, suggesting that the E-UCM be capable of describing the observation that urban areas tend to lose more energy because they retain the process of sensible heating.

Figure 10c presents the difference of individual terms of energy equilibrium over cities with the E-UCM and E-NOU. As the E-NOU uses the model-supplied USGS land-use data, Type 3 (irrigated farmland/grassland) is kept for the urban area selected for the E-UCM, resulting in differences between the two experiments that bear a number of similarities to

those of Fig. 10a, and reflecting, from another point of view, the role of cities in the formation of urban high temperatures and nocturnal heat islands.

5 CONCLUSIONS AND DISCUSSIONS

Based on the introduction of the latest datasets of land use and with the application of the WRF model and its coupled urban canopy model, UCM, a high-temperature weather was numerically simulated that took place in late June through early July 2004, in order to examine, with the WRF/UCM simulation, the formation of urban heat island and urban high-temperature weather.

(1) The E-UCM (with new land-use data and coupled UCM model) has better simulations of the evolution of temperatures at the height of 2 m in urban areas than the E-BPA (with new land-use data and BPA method) and the E-NOU (with old land-use data and coupled UCM model). Compared to the observation, the average absolute error is the smallest with the E-UCM, which is an improvement over the absolute error of both the E-BPA and E-NOU. The improvement is especially good for the nighttime as it is successful in reproducing higher minimum temperatures that are closer to reality; it is particularly essential for the model to simulate the formation of nocturnal heat islands.

(2) The E-UCM-simulated nocturnal heat island is the most intense of all experiments, around 3° C, being the closest to the observation. Nonetheless, although the E-UCM is also successful in simulating relatively high maximum temperatures for the diurnal period of urban areas, they are still lower than the observations.

(3) In addition to the improved simulations of heat island intensity, the E-UCM experiment also simulated how the heat island distributes diurnally in urban areas. Similar to the observations, the heat island characteristics simulated by the E-UCM are well shown in the area from Guangzhou, Foshan through Dongguan.

(4) As shown in an analysis of the difference in energy equilibrium for urban and suburban districts, the better simulation by the E-UCM is attributable to the successful reproduction of the fact that cities absorb more shortwave radiation energy due to low urban reflectivity. Besides, the model is also able to show that high temperatures are likely to appear diurnally in cities as most of the energy input is used in sensible heating, a phenomenon resulting from the lack of evapotranspiration of water vapor. For the nocturnal situation, the model shows that the input of land-surface energy comes from the upward transfer of soil heat flux. Again, because of the small latent heat flux in urban areas, the input energy heats the atmosphere mainly in the form of sensible heat. Due to sustained nocturnal sensible heating, relatively high minimum temperatures are reproduced with distinct heat island features for the urban area.

It is also disclosed in our study that the warming effect induced by the blocking, reflecting and intercepting of longwave and shortwave radiation by buildings, which are taken into account in detailed in the UCM model, is less significant than expected, and the simulated maximum diurnal temperature is still lower than the observation. Relatively intense nocturnal radiation cooling in the urban area may be responsible in some way. Besides, the UCM model in WRFV2.2 is still free of the effect of anthropogenic heat sources, which may affect the intensity of urban heat islands. As shown in existing research, the release of urban anthropogenic heat is one of the important intrigues of intensified heat islands, especially during the night. As what Lin et al.[24] pointed out, such heat release during the night and morning poses the largest influence on the evolution of the boundary layer and heat island intensity. In addressing the same issue, Narumi et al.[25] reported that the magnitude of nocturnal temperarture rise can be nearly three times as high as that of the daytime despite that such heat release is lower during the night than in daytime. All of these issues need to be addressed in future study.

REFERENCES:

[1] ZHOU Shu-zheng, SHU Jiong. Urban Climatology [M]. Beijing: China Meteorological Press, 1994: 572-585.

[2] ZHANG Shang-yin, ZHANG Hai-dong, XU Xiang-de. Climatic character and cause analysis of summer high temperature in main cities of East China [J]. Plateau Meteor., 2005, 24(5): 829-835.

[3] ZHENG Zuo-fang, WANG Ying-chun, LIU Wei-dong. Numerical simulation study for the effects of terrain and land use to summer heat wave in Beijing [J]. J. Trop. Meteor., 2006, 22(6): 672-676.

[4] ZHOU Rong-Wei, JIANG Wei-Mei, HE Xiao-Feng. Numerical simulation of the impacts of the thermal effects of urban canopy structure on the formation and the intensity of the urban heat island [J]. Chin. J. Geophys., 2008, 51(3): 705-715.

[5] MANGLEY G. On the frequency of snowfall in metropolitan England [J]. Quart. J. Roy. Meteor. Soc., 1958, 84: 70-72.

[6] CHANGNON S A. Inadvertent weather modification in urban areas: Lessons for global climate change [J]. Bull. Amer. Meteor., 1992, 73: 619-627.

[7] SHEPHERD J M. A review of current investigations of Urban-induced rainfall and recommendations for the future [J]. Earth Interactions, 2005, 9(12): 1-27.

[8] MASSON V. A physical-based scheme for the urban energy budget in atmospheric models [J]. Bound. Layer Meteor., 2000, 94: 357-397.

[9] KUSAKA H, CHEN F, BAO J W, et al. Simulation of the urban heat island effects over the Greater Houston Area with the high resolution WRF/LSM/Urban coupled system [R]// Symposium on “Planning, Nowcasting, and Forecasting in the Urban Zone”. 1-15 January, 2004, Seattle, WA.

[10] MYRUP L O. A numerical model of the urban heat island

[J]. J. Appl. Meteor., 1969, 8: 908-918.
[11] BORNSTEIN R D. The two-dimensional URBMET urban-boundary layer model [J]. J. Appl. Meteor., 1975, 14: 1459-1477.
[12] VUKOVICH F M, DUNN III J W, CRISSMAN B W. A theoretical study of the St Louis heat island: The wind and temperature distribution [J]. J. Appl. Meteo., 1976, 15: 417-440.
[13] YOSHIKADO H. Numerical study of the daytime urban effect and its interaction with the sea breeze [J]. J. Appl. Meteor., 1992, 31: 1146-1164.
[14] SCHAYES G, THUNIS P, BORNSTEIN R. Topographic vorticity mode mesoscale-β (TVM) model: Part I: Formulation [J]. J. Appl. Meteor., 1996, 35: 1815-1823.
[15] ROZOFF C, COTTON W R, ADEGOKE J O. Simulation of St Louis, Missouri, land use impacts on thunderstorms.[J]. J. Appl. Meteor., 2003, 42: 716-738.
[16] NIYOGI D, HOLT T, ZHONG S, et al. Urban and land surface effects on the 30 July 2003 MCS event observed in the Southern Great Plains [J]. J. Geophys. Res., 2006, 111, D19107, doi:10.1029/2005JD006746.
[17] CHIN H N S, LEACH M J, SUGIYAMA G A, et al. Evaluation of an urban canopy parameterization in a mesoscale model using VTMX and URBAN 2000 Data [J]. Mon. Wea. Rev., 2005, 133(7): 2043-2068.
[18] XIE Shan-ju, HUANG Wei-feng. The urban high temperature in Guangzhou and its relief [J]. Trop. Geograph., 1996, 16(4): 340-344.
[19] LU Shan, YE Meng. The research on relationship between outer circulation of tropical cyclones and high temperature weather in Guangzhou [J]. J. Trop. Meteor., 2006, 22(5): 461-465.
[20] JI Zhong-ping, LIN Gang, LI Xiao-juan, et al. High temperature anomalies in Guangdong in summer 2003 and its climatic background [J]. J. Trop. Meteor., 2005, 22(2): 207-216.
[21] MENG Wei-guang, YAN Jing-hua, HU Hai-bo. Urban effect and summertime thunderstorms in Guangzhou under the backgroundof tropical cyclones [J]. Sci. in China (Ser. D: Earth Sci.), 2007, 37(12): 1660-1668.
[22] KUSAKA H, KIMURA F. Coupling a single-layer urban canopy model with a simple atmospheric model: Impact on urban heat island simulation for an idealized case [J]. J. Meteor. Soc. Japan, 2004, 82: 67-80.
[23] OKE T R. The energetic basis of the urban heat island [J]. Quart. J. Roy. Meteor. Soc., 1982, 108: 1-24.
[24] LIN C Y, CHEN F, HUANG H, et al. Urban heat island effect and its impact on boundary layer development and land-sea circulation over Northern Taiwan [J]. Atmos. Environ., 2008, 42: 5639-5649.
[25] NARUMI D, KONDO A, SHIMODA Y. Effects of anthropogenic heat release upon the urban climate in a Japanese megacity [J]. Environ. Res., 2009, 109: 421-431.

Citation: MENG Wei-guang, ZHANG Yan-xia, LI Jiang-nan et al. Application of WRF/UCM in the simulation of a heat wave event and urban heat island around Guangzhou. *J. Trop. Meteor.*, 2011, 17(3): 257-267.